Decay of Turbulence at High Reynolds Numbers

Michael Sinhuber, Eberhard Bodenschatz, and Gregory P. Bewley[*]
Max Planck Institute for Dynamics and Self-Organization, 37077 Göttingen, Germany
(Received 3 July 2014; published 23 January 2015)

Turbulent motions in a fluid decay at a certain rate once stirring has stopped. The role of the most basic parameter in fluid mechanics, the Reynolds number, in setting the decay rate is not generally known. This Letter concerns the high-Reynolds-number limit of the process. In a classical grid-turbulence wind-tunnel experiment that both reaches higher Reynolds numbers than ever before and covers a wide range of them ($10^4 < \mathrm{Re} = UM/\nu < 5 \times 10^6$), we measure the decay rate with the unprecedented precision of about 2%. Here U is the mean speed of the flow, M is the forcing scale, and ν is the kinematic viscosity of the fluid. We observe that the decay rate is Reynolds-number independent, which contradicts some models and supports others.

Turbulence dissipates kinetic energy, and the easiest way to see this is to let turbulence freely decay, by removing the agitation that initially set the fluid in motion. In so doing, one observes qualitatively that the fluid comes to rest. The rate at which this happens is the subject at hand, and underlies general turbulence phenomena and modeling. To simplify the problem, the statistics of the turbulent fluctuations are often arranged to be spatially homogeneous and isotropic [1,2]. Even under these conditions, it is not possible quantitatively to predict the decay rate; it is even difficult precisely to measure the decay rate [3–6]. Yet empirical constraints on the properties of decaying turbulence are what is needed to advance the knowledge of the subject.

The physics that control the decay are not fully understood, to the extent that the role of the most basic parameter in fluid mechanics, the Reynolds number, is not clear. What is known is that toward very low Reynolds numbers, the decay rate increases [7,8], as it also does when the spatial structure of the turbulence grows to the size of its container [4,9]. Here, we study the rate of decay in the limit of large Reynolds numbers for turbulence free from boundary effects, a rate which cannot be determined from previous data.

One theoretical framework predicts that the decay rate depends on the large-scale structure of the flow, and not on the Reynolds number once turbulence is fully developed [2,10–13]. As the Reynolds numbers diverge to infinity, the scale at which energy is dissipated grows arbitrarily small, but these scales continue to dissipate energy as quickly as it is transferred to them by the large scales. This picture is compatible with an emerging consensus that the initial structure of the turbulence sets its decay rate, even when the flow is homogeneous [14–17].

There is also, however, a line of thinking that an elegant and fully self-similar decay emerges in the limit of high Reynolds number [14,15,18–23]. In this description,

turbulence tends to become statistically similar to itself, when appropriately rescaled, even as it decays. Observation of a tendency toward slower decay with increasing Reynolds numbers would support this view [14,21–23]. Our data, however, do not show this tendency.

The issue is of practical consequence because decaying turbulence is a benchmark for turbulence models [8,24–26]. Not only this, but both simulations and experiments can be performed easily at low Reynolds numbers, say $\mathrm{Re} < 10^5$; how well can their findings describe the high-Reynolds number flows that exist in nature, where often $\mathrm{Re} > 10^6$? Our experiments bridge this gap, and also contribute to a basic understanding of the nature of turbulence. The objectives are similar to those in other recent programs in fluid mechanics, where asymptotic scaling behavior was sought in other types of flows [27,28].

According to dimensional reasoning, it is useful to think of physical laws in terms of dimensionless numbers [29]. In turbulence, these numbers include the Reynolds number Re and a family of others that describe the initial and boundary conditions (BCs) of the flow. Some set of these numbers might control the decay of the turbulence. To isolate Re effects in our experiment, we held fixed the other numbers. That is, we fixed the BCs so that the large-scale structure of the flow was approximately fixed. We then changed Re by varying the viscosity of the fluid [30]. The ability to do this was almost unique among turbulence decay experiments, and made it possible both to cover a wider range and to reach higher Re than ever before. In previous experiments, changes to the BCs and to Re were made together, which conflated Re effects with those arising from changes in the large-scale structure of the flow.

Our experiment was based on a tradition established by early pioneers of using wind tunnels with grids in them as instruments to discover empirically how turbulence decays [31–33]. Grids placed at one end of the tunnel stir up the flow as it passes through them, so that grid turbulence can

be thought of as the canonical wake flow. Grids with different geometries produce turbulence with different structure, and recent work has focused on the turbulence downstream of grids with novel geometries [5,17,34,35]. We used a single classical grid to isolate the effects of Re from those of the geometry, and to compare our results with those from 80 years of turbulence research in wind tunnels.

We performed the experiments in the Variable Density Turbulence Tunnel (VDTT) [30]. The VDTT circulated both air and pressurized sulfur-hexafluoride. The Reynolds number was adjusted by changing the pressure of the gas, which changes its kinematic viscosity. Turbulence was produced at the upstream end of the 8.8 m long upper test section by a classical grid, that is, by a biplanar grid of crossed bars with square cross section. The mesh spacing M of the grid was 0.18 m, and the projected area of the grid was 40% of the cross section of the tunnel. A linear traverse positioned probes at 50 logarithmically spaced distances x between 1.5 and 8.3 m downstream of the grid. A Galilean transformation converts the distances from the grid into the time over which the turbulence decayed, so that $t = x/U$. Here U is the mean speed of the flow down the tunnel, which was about 4.2 m/s for most experiments.

We used hot-wire probes to obtain long traces of the component of the velocity aligned with the mean flow. At each of 50 distances from the grid we acquired 5 min of data. The experiment was repeated at 36 Reynolds numbers and with three probes, for a total of about 10^8 integral lengths of data. We used classical hot wires produced by Dantec Dynamics from both 1.25 mm lengths of 5 μm wire, dubbed the P11 probe, and from 450 μm lengths of 2.5 μm diameter wire, dubbed the Mini probe, as well as the new nano-scale thermal anemometry probe (NSTAP) developed at Princeton that is just 60 μm long [36,37]. The probes were approximately at the centerline of the tunnel, with the P11 probe downstream of a grid bar, the Mini probe behind the edge of a grid bar, and the NSTAP probe between grid bars. The small differences between the results given by different probes do not affect the conclusions of this Letter, and will be the subject of a future detailed report.

Figure 1(a) shows for several Reynolds numbers the normalized turbulent kinetic energy as a function of the time since the flow passed through the grid. The variance of the velocity, u^2, is proportional to the total kinetic energy in the turbulent fluctuations, and we refer in this Letter to u^2 as the kinetic energy itself. This is because the total mass of the fluid was fixed, because grid turbulence is nearly isotropic, and because the residual anisotropy decays much more slowly than the energy [6,15,17,23,38]. The solid curve, the master curve, is the mean of 99 decay curves accumulated by all three probes at all Reynolds numbers. The decay curves are remarkably similar to each other, even though their Reynolds numbers span more than 2 orders of magnitude.
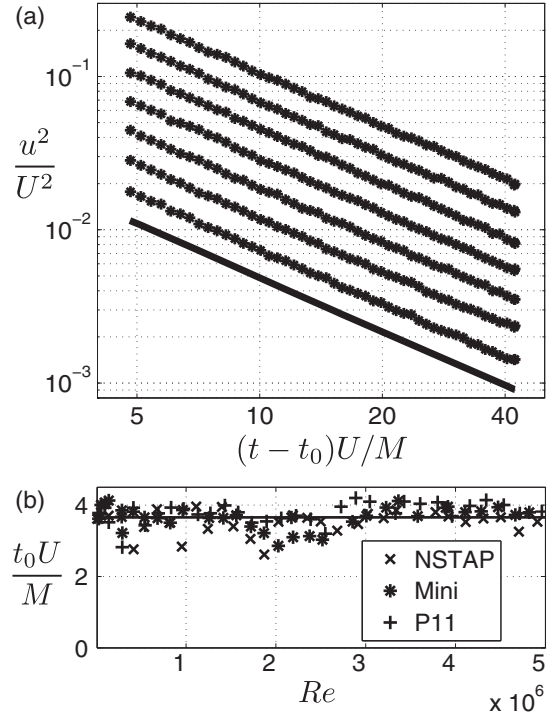

FIG. 1.   (a) The decay of the turbulent kinetic energy u^2 for seven representative Reynolds numbers as a function of time. The linear relationship between the data on the double-logarithmic scales of the figure indicates a power law dependence on time. The values of Re $\times 10^{-3}$ for each set of data were 26, 54, 140, 410, 820, 1700, 3200, and 4800 from bottom to top. Each set of data is shifted upward to separate it from the lowest curve, which is unshifted. The lowest curve, the master curve, is the mean of 99 sets of data acquired at different Reynolds numbers. We normalized the kinetic energy by that in the mean flow, U^2, and time by M/U. Time was offset by t_0, the virtual origin. (b) We found the virtual origin by fitting each decay curve to a power law as described in the text. Over the full range of Reynolds numbers, the virtual origin fluctuated with a standard deviation of less than 10% of its mean value of $t_0 U/M = 3.66$.

We see in Fig. 1(a) that the data follow straight lines, which is to say that they obey power laws of time

$$\frac{u^2}{U^2} = C\left((t - t_0)\frac{U}{M}\right)^n, \qquad (1)$$

where n quantifies the decay rate that is the subject of this Letter. The time origin t_0 for the power law, called the virtual origin, is not directly measurable and needs to be determined by some means. One way to do this is by a three-parameter fit of the data to Eq. (1) using a nonlinear least-squares algorithm [39]. However, the uncertainties in t_0 and n are coupled, leading to unreliable estimates of these parameters [3–6]. We describe two ways to avoid this difficulty below, though the conclusions of the Letter are not sensitive to the method of analysis.

Figure 1(b) shows that the virtual origin, to a first approximation, was Re independent. Its value is probably connected to the development of the wakes behind the bars that compose the grid; in previous experiments different grid geometries produced different virtual origins [15,17,40]. The wakes behind square bars are nearly Re independent in the Re regime of our experiments, and do not show the drag crisis characteristic of circular cylinders [41]. It therefore seems reasonable to assign a fixed value to the virtual origin.

With the virtual origin fixed to its mean value $t_0 U/M = 3.66$, we could measure the decay exponents more precisely with a two- (rather than a three-) parameter fit of the data to Eq. (1). Here, C and n were free parameters, and we use the power law as a tool to uncover the Re evolution of the decay process.

Figure 2 shows our measurements of the decay exponents and compares them to those in the literature. Our data neither approach $n = -1$ nor trend toward a slower decay with increasing Re, despite the wide range of high Re achieved in the VDTT. Combining all our data, we obtain a mean decay exponent of $n = -1.18 \pm 0.02$, close to Saffman's prediction of -1.2 [10].

Our second method of analysis emphasizes the Re variation of the decay rate, rather than its specific form. We make the ansatz that the kinetic energy decay at one Reynolds number $E_i(t, \mathrm{Re}_i)$ is a power law function of the decay at another Reynolds number $E_j(t, \mathrm{Re}_j)$, so that $E_j \sim E_i^{\Delta n}$, and Δn is a relative decay exponent. Such a relationship does not strictly require power-law evolution of the energies, E_i or E_j [58]. If, however, such a power-law decay does hold, as in our experiment, then $\Delta n = n_j/n_i$,

where n_i and n_j are the decay exponents at the two Reynolds numbers. Note that the variation in the virtual origin must be small relative to its mean, as it was in our experiment. In practice, we took E_i to be the master curve shown in Fig. 1(a) and E_j to be the decay of u^2 at the various Re, and we extracted values of Δn by fitting power laws to graphs of E_j against E_i. The advantage was not only that the ambiguity of finding the virtual origin was eliminated, but the requirement of power-law decay was relaxed.

The inset of Fig. 2 presents the relative scaling exponents derived by the above procedure. Here, a trend toward a slower decay would appear as a tendency of the data toward lower values with increasing Re. Again, the data show no such trend and scatter around 1.0, which means that the dominant behavior is for the decay not to change with increasing Re.

Different conclusions may be drawn from the previous data gathered in Fig. 2. An approach to an $n = -1$ decay might be seen in the green diamonds [14,40], while the blue squares may be consistent with no change [48]. In computer simulations [22,59,60], the decay slowed down slightly with increasing Re, but with similar reach in Re and scatter in the exponents as in previous experiments. All in all, this scatter is significant, and may be attributable to variations in initial and boundary conditions between experiments, that is, to the geometry of the grids used or to other variations in the experimental design. The results from some experiments are not shown either because the form of the decay was not a power law or because the exponents fell out of the range of the plot. Collectively, the previous data leave open the question of how the decay rate behaves in the limit of large Re.
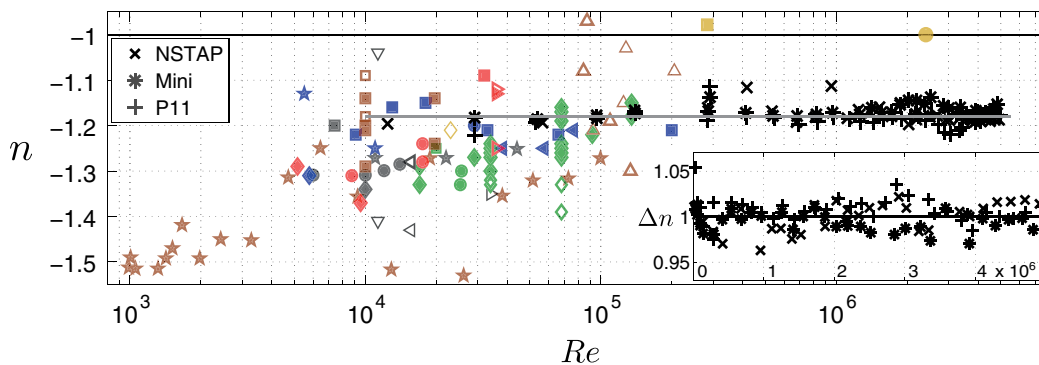

FIG. 2 (color online).   The exponents n in Eq. (1) of power-law fits to the data quantify the energy decay rate. The line is a fit to our data ($\times$, $*$, $+$), for which the mean decay rate was $n = -1.18$ with a standard deviation of 0.02. The 95% confidence interval for each value of n ($\pm 0.9\%$) is given approximately by the size of the symbols. Additional data drawn from the literature appear as follows. Stars: brown [23], blue [33], gray [42]. Diamonds: red [43], blue [44], black [45], green [40], yellow [46]. Squares: black [47], blue [48], brown [15], green [49], red [50], yellow [51]. Circles: black [3], red [52], blue [53], green [54], yellow [55]. Triangles: pointing down [56], black pointing left [57], red [38], blue [34], brown [17]. Closed symbols mark experiments that employed classical grids, as ours did, whereas open symbols mark those that employed modified grids such as fractal grids. Symbols with thin lines mark active-grid experiments. In some of these experiments, modifications to the grids were made deliberately to elicit changes in the decay [15,17]. The inset shows on a linear scale of Re the relative decay exponents as described in the text. Our data reveal that the rate of decay is invariant with respect to the Reynolds number for Re $\gg 10^4$.

Because the Reynolds number seemed not to govern the decay rate in our experiment, we sought an explanation of the decay in terms of the large-scale structure of the flow. One way to derive predictions is to consider the evolution equation for the kinetic energy in freely decaying turbulence: $(3/2)du^2/dt = -\epsilon$. In the classical description, the dissipation rate ϵ is independent of Re so that $\epsilon = C_\epsilon u^3/L$, and $(3/2)du^2/dt = -C_\epsilon u^3/L$. The constant C_ϵ is of order 1 in most flows [61] and it was also in our experiment, varying over time by about 4%.

In order to integrate the energy equation, some relationship between the energy u^2 and the correlation length L must be derived. Typically, this relationship is a power law $L \sim (u^2)^m$ with $m = -1/2$, $-1/3$, and $-1/5$, for each of the self-similar, Saffman, and Kolmogorov theories, respectively [2,10,18]. Yet other exponents can be supported by different arguments [11,12]. Integration of the energy equation then yields predictions for the decay law $u^2 \sim t^n$, with $n = -1$, $-6/5$ and $-10/7$, for the three theories, respectively, and $n = 2/(2m - 1)$ generally [6]. Fortunately, it is possible to look directly for a relationship between u^2 and L, without the ambiguity of determining a virtual origin, since the virtual origin must be a property of the flow and so must be the same for all of its statistics.

Figure 3 shows the correlation length L calculated from the scale r at which the velocity correlation function dropped below $1/e$. The velocity correlation function was $f(r) = \langle u(x)u(x + r)\rangle_x/u^2$, which could be calculated from our time series of velocity in the usual way through Taylor's hypothesis [62]. Gray symbols mark our data, whereas the solid lines denote the various theoretical predictions. Neither Kolmogorov's nor the self-similar decay agrees with our data, whereas Saffman's prediction is consistent with our data for large u^2/U^2.

Where the data are approximately straight in Fig. 3, a power-law fit yields $m = -0.35$ so that the theory predicts $n = 2/(2m - 1) = -1.18$, which is precisely what we measured directly from the decay of kinetic energy. We attribute the deviations from Saffman's prediction at large times to confinement of the flow by the walls of the tunnel [4,9].

Saffman's theory follows the lines of Kolmogorov's but is based on a different invariant, for which we now give a brief physical interpretation. We first picture turbulence as a sea of vortices that each carry both linear and angular impulses [63]. The vortices interact as the turbulence evolves, and while their kinetic energies decay, their linear and angular impulses are conserved. The conservation of their linear impulses is embodied in Saffman's invariant [64,65]. This invariant yields the relationship between u^2 and L mentioned above, and so to the $-6/5$th decay law [10]. In the case that the linear impulses of the vortices are initially small compared with their angular impulses, the character of the decay is dominated by the conservation of the latter, which is embodied in Loitsyanskii's invariant
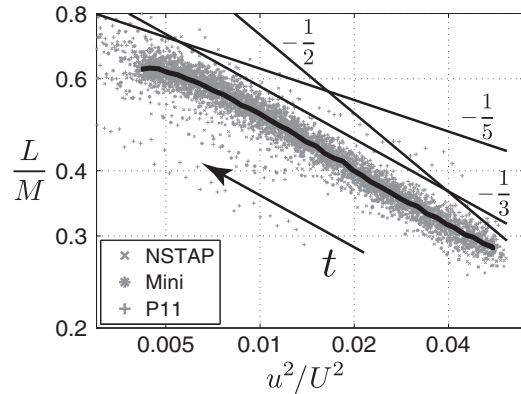

FIG. 3. The correlation lengths L were approximately a power law of the kinetic energy u^2 during the decay. Time proceeds from right to left in the graph, as indicated by the arrow. Here we combined all data without discrimination since there was no trend with respect to Re. To produce the smooth curve, we took the median values of L/M and u^2/U^2 data falling within logarithmically spaced bins in u^2/U^2. The relationships posited by well-known theories are indicated by straight lines. Our data are consistent with Saffman's theory, with slope $-1/3$.

[66] and Kolmogorov's faster $-10/7$th decay law [2]. Since both invariants are insensitive to the small-scale structure of the flow, their respective decay laws are Re independent. One finds that turbulence is more durable when its constituent vortices carry significant linear impulse in addition to their angular impulse.

In summary, we observed the decay rate of turbulence to be Reynolds number independent, and the decay to proceed in a way consistent with Saffman's predictions [10]. The data do not agree with the predictions of Kolmogorov, Dryden, George, Speziale, Bernard, and others [2,14,18,21]. Initial or boundary conditions different from ours, established for instance by active or fractal grids [34,46], may produce different decay rates and even different Re dependencies. Our data, however, indicate that the self-similar decay is probably not the generic high-Re decay. We attribute the residual Re dependencies in our data to minor Re variations in the flow around the grid, and not to an effect of Re on the physics of the ensuing decay. In closing, we note that a deeper understanding of the decay mechanisms may be acquired by looking at different systems. Quantum turbulence, for example, whose small-scale physics are completely different, may have the same large-scale structure as classical turbulence and may decay in the same way [9,67].

*gregory.bewley@ds.mpg.de

[1] T. von Kármán and L. Howarth, Proc. R. Soc. A **164**, 192 (1938).

[2] A. N. Kolmogorov, Dokl. Akad. Nauk SSSR **31**, 538 (1941).

[3] M. S. Mohamed and J. C. LaRue, J. Fluid Mech. **219**, 195 (1990).

[4] L. Skrbek and S. R. Stalp, Phys. Fluids **12**, 1997 (2000).

[5] D. Hurst and J. C. Vassilicos, Phys. Fluids **19**, 035103 (2007).

[6] P. A. Krogstad and P. A. Davidson, J. Fluid Mech. **642**, 373 (2010).

[7] S. C. Ling and T. T. Huang, Phys. Fluids **13**, 2912 (1970).

[8] J. B. Perot and S. M. de Bruyn Kops, J. Turbul. **7**, N69 (2006).

[9] S. R. Stalp, L. Skrbek, and R. J. Donnelly, Phys. Rev. Lett. **82**, 4831 (1999).

[10] P. G. Saffman, Phys. Fluids **10**, 1349 (1967).

[11] G. L. Eyink and D. J. Thomson, Phys. Fluids **12**, 477 (2000).

[12] P. A. Davidson, Phys. Fluids **23**, 085108 (2011).

[13] M. Meldi, P. Sagaut, and D. Lucor, J. Fluid Mech. **668**, 351 (2011).

[14] W. K. George, Phys. Fluids A **4**, 1492 (1992).

[15] P. Lavoie, L. Djenidi, and R. A. Antonia, J. Fluid Mech. **585**, 395 (2007).

[16] P. C. Valente and J. C. Vassilicos, Phys. Lett. A **376**, 510 (2012).

[17] A. Thormann and C. Meneveau, Phys. Fluids **26**, 025112 (2014).

[18] H. L. Dryden, Q. Appl. Math. **1**, 7 (1943).

[19] C. C. Lin, Proc. Natl. Acad. Sci. U.S.A. **34**, 540 (1948).

[20] J. O. Hinze, *Turbulence* (McGraw-Hill, New York, 1975).

[21] C. G. Speziale and P. S. Bernard, J. Fluid Mech. **241**, 645 (1992).

[22] P. Burattini, P. Lavoie, A. Agrawal, L. Djenidi, and R. A. Antonia, Phys. Rev. E **73**, 066304 (2006).

[23] T. Kurian and J. H. M. Fransson, Fluid Dyn. Res. **41**, 021403 (2009).

[24] W. K. George, H. Wang, C. Wollblad, and T. G. Johansson, in *14th Australasian Fluid Mechanics Conference* (Adelaide University, Adelaide, 2001), pp. 41–48.

[25] J. R. Hughes, L. Mazzei, A. A. Oberai, and A. A. Wray, Phys. Fluids **13**, 505 (2001).

[26] H. S. Kang, S. Chester, and C. Meneveau, J. Fluid Mech. **480**, 129 (2003).

[27] X. He, D. Funfschilling, H. Nobach, E. Bodenschatz, and G. Ahlers, Phys. Rev. Lett. **108**, 024502 (2012).

[28] S. G. Huisman, D. P. M. van Gils, S. Grossmann, C. Sun, and D. Lohse, Phys. Rev. Lett. **108**, 024501 (2012).

[29] E. Buckingham, Phys. Rev. **4**, 345 (1914).

[30] E. Bodenschatz, G. P. Bewley, H. Nobach, M. Sinhuber, and H. Xu, Rev. Sci. Instrum. **85**, 093908 (2014).

[31] L. F. G. Simmons and C. Salter, Proc. R. Soc. A **145**, 212 (1934).

[32] H. L. Dryden, G. B. Schubauer, W. C. Mock, and H. K. Skramstad, Tech. Rep. No. 581, NACA, 1936.

[33] G. K. Batchelor and A. A. Townsend, Proc. Roy. Soc. A **193**, 539 (1948).

[34] P. C. Valente and J. C. Vassilicos, J. Fluid Mech. **687**, 300 (2011).

[35] P. A. Krogstad and P. A. Davidson, Phys. Fluids **24**, 035103 (2012).

[36] S. C. C. Bailey, G. J. Kunkel, M. Hultmark, M. Vallikivi, J. P. Hill, K. A. Meyer, C. Tsay, C. B. Arnold, and A. J. Smits, J. Fluid Mech. **663**, 160 (2010).

[37] M. Vallikivi, M. Hultmark, S. C. C. Bailey, and A. J. Smits, Exp. Fluids **51**, 1521 (2011).

[38] P. A. Krogstad and P. A. Davidson, J. Fluid Mech. **680**, 417 (2011).

[39] J. J. Moré, in *Numerical Analysis* (Springer, New York, 1978), pp. 105–116.

[40] G. Comte-Bellot and S. Corrsin, J. Fluid Mech. **25**, 657 (1966).

[41] G. Schewe, Tech. Rep., Deutsche Forschungs-und Versuchsanstalt für Luft-und Raumfahrt, 1984.

[42] L. A. Wyatt, Ph.D. thesis, University of Manchester, 1955.

[43] A. Sirivat and Z. Warhaft, J. Fluid Mech. **128**, 323 (1983).

[44] K. Yoon and Z. Warhaft, J. Fluid Mech. **215**, 601 (1990).

[45] Z. Warhaft and J. L. Lumley, J. Fluid Mech. **88**, 659 (1978).

[46] L. Mydlarski and Z. Warhaft, J. Fluid Mech. **320**, 331 (1996).

[47] K. R. Sreenivasan, S. Tavoularis, R. Henry, and S. Corrsin, J. Fluid Mech. **100**, 597 (1980).

[48] C. M. White, A. N. Karpetis, and K. R. Sreenivasan, J. Fluid Mech. **452**, 189 (2002).

[49] R. A. Antonia, R. J. Smalley, T. Zhou, F. Anselmet, and L. Danaila, J. Fluid Mech. **487**, 245 (2003).

[50] E. van Doorn, C. M. White, and K. R. Sreenivasan, Phys. Fluids **11**, 2387 (1999).

[51] G. P. Bewley, D. P. Lathrop, L. R. M. Maas, and K. R. Sreenivasan, Phys. Fluids **19**, 071701 (2007).

[52] M. S. Uberoi and S. Wallis, J. Fluid Mech. **24**, 539 (1966).

[53] C. W. Van Atta and W. Y. Chen, J. Fluid Mech. **34**, 497 (1968).

[54] M. S. Uberoi, Phys. Fluids **6**, 1048 (1963).

[55] A. L. Kistler and T. Vrebalovich, J. Fluid Mech. **26**, 37 (1966).

[56] R. E. G. Poorte and A. Biesheuvel, J. Fluid Mech. **461**, 127 (2002).

[57] H. Makita, Fluid Dyn. Res. **8**, 53 (1991).

[58] R. Benzi, S. Ciliberto, C. Baudet, and G. R. Chavarria, Physica D (Amsterdam) **80**, 385 (1995).

[59] T. Ishida, P. A. Davidson, and Y. Kaneda, J. Fluid Mech. **564**, 455 (2006).

[60] J. B. Perot, AIP Adv. **1**, 022104 (2011).

[61] K. R. Sreenivasan, Phys. Fluids **10**, 528 (1998).

[62] G. I. Taylor, Proc. R. Soc. A **164**, 476 (1938).

[63] P. A. Davidson, *Turbulence: An Introduction for Scientists and Engineers* (Oxford University Press, New York, 2004).

[64] G. Birkhoff, Commun. Pure Appl. Math. **7**, 19 (1954).

[65] P. G. Saffman, J. Fluid Mech. **27**, 581 (1967).

[66] L. G. Loitsyanskii, Trudy TsAGI **440**, 3 (1939).

[67] L. Skrbek and K. R. Sreenivasan, Phys. Fluids **24**, 011301 (2012).